RSC Advances

ROYAL SOCIETY OF CHEMISTRY

www.rsc.org/advances

CO_2 Adsorption on Single-Walled Boron Nitride Nanotubes Containing Vacancy Defects

Edson Nunes Costa Paura[a], Wiliam F. da Cunha[a], Luiz Fernando Roncaratti[a], João B. L. Martins[b], Geraldo M. e Silva[a], and Ricardo Gargano[c],[a]
[a] *Institute of Physics, University of Brasilia, CP 4455, 70919-970, Brazil,*
[b] *Institute of Chemistry, University of Brasilia, CP 4478, 70904-970, Brazil. and*
[c] *Departments of Chemistry and Physics, Quantum Theory Project, University of Florida, Gainesville, Florida 32611.*
(Dated: February 9, 2015)

The adsorption of CO_2 molecule on vacancy defect type of armchair (5,5) and zigzag (10,0) single walled boron nitride nanotubes was studied based on Density Functional Theory (DFT). Vacancy defects were studied and the geometrical modifications implemented on the original hexagonal lattice yielded a considerable level of changes on the electronic properties. These changes reflect in a greater level of CO_2 reactivity in relation to the adsorption over pristine structure. For all types of studied CO_2 molecule interaction, we have found a chemical adsorption process based on binding energy. Furthermore, the CO_2 adsorption takes place on the top of vacancy region. It was observed a decomposition state when the CO_2 molecule interacts with the armchair nanotube with a vacancy on the nitrogen site. By comparing values of adsorption energies with those from other defect approaches present in the literature, we conclude that the proposed protocol presents a possible tool to develop stable and sensible carbon dioxide sensors.

Keywords: boron nitride nanotubes, CO_2 molecule, vacancy defect, density functional theory.

I. INTRODUCTION

Boron nitride nanotubes (BNNTs) were first predicted in the mid 90's through tight binding calculations, and synthesized shortly after that by means of a arc-discharge method[1,2]. Since the advent of these studies, several theoretical and experimental investigations concerning the properties of these novel materials have been carried out[3,4]. These efforts, together with the many advantages these materials present, have turned BNNTs in fundamental tools for the nanotechnology field. Among these advantages, the fact that BNNTs tends to present an indirect band gap greater than 2eV, regardless of the geometrical parameters considered[1]. Also, these materials present a great chemical stability[5], an excellent mechanical resistance[6], high thermal conductivity[7] and considerable resistance to both heat and electric currents[8]. Indeed, these features have turned BNNTs into even more interesting materials than their carbon counterparts[9], as far as gas sensor technology and other kinds of nanotechnology uses is concerned.

All the aforementioned advantages are known to be valid for ideal nanotubes, i.e., structures which are defect free. In the actual process of fabrication, however, defects that are either spontaneously or artificially produced may alter physical and electronic properties of BNNTs. These properties changes might lead to effects that can alternatively limit or enhance the applicability of these structures. In this sense, one of the early works of this field has shown that mechanically induced defects lead to the formation and dislocation of dipoles on BNNT walls, provided certain conditions of temperature and pressure are considered[10]. Similarly, another work, that considered transition electronic microscopy (TEM) together with theoretical modeling, suggested that defects created through electronic irradiation are mainly of a divacancy nature. This study also has shown that the set of several vacancies induces the creation of extended defects, that locally alter the nanotube diameter and chirality, thus affecting their electronic and optical properties[11]. TEM is an appropriate experimental apparatus for imaging defective structures and also for inducing in situ the appearance of defects. By using energetic electrons (100keV), this technique is capable of removing single atoms from lattice through direct knock-on collisions[11]. Interesting signatures of point defects (such as single vacancies), can be seen in the high-resolution electron microscopy images of a bundle of BNNTs taken after being irradiated by an energetic electron beam[11]. Activated boron nitride as an effective adsorbent for metal ions and organic pollutants has been also studied in the literature[12].

Some relevant theoretical works also propose that the presence of vacancies raises the concentration of electrons or holes depending if the defect is produced in the boron or in the nitrogen atom sites[13]. Likewise, a recent work by Li *et al.*[14] shows that a charge redistribution takes place near the defect site on the wall of a armchair BNNT so that this effect might increase the chemical reactivity of BNNTs regarding the capture of molecular species. Moreover, there is an urgent need of new carbon dioxide capture strategies. Therefore, a systematic investigation on the role played by vacancy type defects on favoring the capture of CO_2 is highly desired. The importance of this particular molecule lies in fact that CO_2 is one of the main anthropic greenhouse gases, thus dangerously inducing severe climate changes[15].

Recently, a theoretical study based on Density Functional Theory (DFT) calculations has shown that a single graphene-like hexagonal BN sheet endowed with a vacancy on the boron site, could efficiently capture a carbon dioxide molecule[16]. It was reported that in one of the steps of the adsorption process, the CO_2 was broken into an oxygen molecule and a carbon atom captured by the lattice. This step is observed to take place through an intermediate chemisorption state on the defective BN sheet. Therefore, we make use of single walled armchair (henceforward BNNT(5,5)) and zigzag (BNNT(10,0)) boron nitride nanotubes to investigate the influence of nitrogen or boron sites on the CO_2 molecule reactivity. Specifically, the main question is regarding the chiral angle effects as well as the influence on the CO_2 adsorption process due to the defect site.

The remainder of this work is organized as follows: section II presents the computational settings, followed by our results and their discussions in section III; we summarize the main features of this work in section IV.

II. COMPUTATIONAL DETAILS

Density functional theory calculations of CO_2 adsorption were carried out on infinitely large boron nitride nanotubes by means of the DMol^3 code[17,18] to compute equilibrium geometries, total energies, charge analysis and electronic densities. Electronic exchange correlation was treated within the generalized gradient approximation (GGA)[19] with the PW91 functional[20]. The PW91 functional was recently used to study the interaction of BNNT with gas molecules[21].

The positions of all the atoms were fully relaxed until the following convergence criteria were met: 0.001 Ha/Å for the force constant and 0.003 Å for displacement. The self-consistent field computations criterion was chosen to be 10^{-6} Ha. The electronic wave functions were expanded in a 4.4 version double numerical plus polarization basis set (DNP) truncated at a real space cut-off of 4.1 Å. DNP basis set was found to lead to small Basis set superposition error (BSSE) (about 1.62 kJ/mol)[22]. Therefore, we have used BSSE correction. Due to the presence of boron and nitrogen atoms in the model, all calculations were spin unrestricted. A 0.005 Ha smearing[23] and 6 Pulay direct inversion of the iterative subspace (DIIS)[24] was applied to the system to facilitate convergence of the electronic structures.

It must be noted that BNNTs used in nanotechnology applications were known to be of very large length. However, the explicit consideration of such a large system tends to be computationally expensive. In order to surpass this difficulty, whereas treating the system in a suitable approach, the 3D periodic boundary conditions were applied to the whole system, accomplishing to simulate the infinitely large BNNTs. The size of the vacuum space in-between two neighbor image tubes was set to be 20Å to prevent the interaction between the atoms of each unit cell. The Brillouin zone for a single cell was sampled by 1x1x11 special k-points.

In order to compute the adsorption energy[25], we make use of the total energy of the isolated BNNT (E_{BNNT}), of the CO_2 molecule energy (E_{CO_2}), as well as of the energy of the complex system composed of the gas molecule interacting with the nanotube ($E_{BNNT+CO_2}$). The equation below employs these terms in the calculation of the adsorption energy

$$E_{ads} = E_{BNNT+CO_2} - E_{BNNT} - E_{CO_2}.$$

It is important to remark that a negative (positive) E_{ads} denote exothermic (endothermic) adsorption. The E_{ads} values and other properties are calculated based only on the lowest-energy structural configuration for the CO_2/BNNT systems. In this work, the charge distribution on the system was analyzed by the Mulliken population method[26], despite its known limitations, since our interest was to analyze the trend of charge distribution across the same models.

Our work concerns the influence of the vacancy defects of BNNTs and of their chiralities over the CO_2 adsorption process. In other words, we compare the adsorption of the gas molecule with and without structural defects for two different symmetries.

III. RESULTS AND DISCUSSIONS

In order to better present our simulation results we divided the present section in three subsections. The first one (III A) treats the interaction of pristine nanotubes interacting with a CO_2 molecule. Subsection III B regards the effects of a vacancy type on the properties of the nanotube itself. Finally, subsection III C treats the adsorption process of the CO_2 molecule on vacancy endowed nanotubes.

A. Pristine BNNTs interacting with CO_2

Throughout the work we adopted single walled boron nitride nanotubes of the zigzag (5,5) and armchair (10,0) chiralities. We first take into account the interaction of a CO_2 molecule on a defect free nanotube for means of future comparison. Consequently, we can observe the effect of vacancy defect over the gas adsorption. We begin by separately performing the geometry optimization of a nanotube of each chirality. This was accomplished through the use of the DMol3 package by considering a total of 60 atoms for the BNNT(5,5), and of 80 atoms for the BNNT(10,0) together with periodic boundary conditions in order to mitigate border effects. It was obtained a B—N length of approximately 1.450 Å for the pristine nanotubes, regardless their chirality. The free CO_2 molecule achieved a typical linear structure with a C—O bonding length of 1.166 Å.

As a next step, we placed the CO_2 molecule in the neighborhood of pristine BNNTs, and carried out a geometry optimization. Figure 1 presents the frontal and side view of the equilibrium configuration for the two different nanotube chiralities considered. One can observe that, regardless the chirality, both the BNNTs and the CO_2 molecule preserve their original geometrical characteristics. For the case of BNNT (5,5), the CO_2 molecule configuration was parallel to the tube axis and located outside the BNNT well, with its carbon atom directly in front of the nitrogen atom of the BNNT, and its oxygen atoms close to the boron atoms of the BNNT.

This behavior can be understood in terms of the polar character of the B—N bonding, which creates a higher charge concentration over the nitrogen atoms, due to the greater nitrogen electronegativity when compared to boron. Thus it is expected that the CO_2 atoms are organized by means of electronic affinity: the carbon atom of the carbon dioxide is positively polarized by the nitrogen atom whereas the oxygen atoms by the boron of the nanotubes.

As for the BNNT (10,0), it was calculated the CO_2 molecule above the center of a nanotube hexagon. This configuration was achieved after the molecule performing a 38^o rotation related to its original position around its axis, with its oxygen atoms directly above the nanotube boron atoms. In this case, as in previous reported works[27], the zigzag bonding pattern of the B—N plays an important role over the molecule orientation related to the tube axis.

Table I presents the adsorption energies (E_{ads}), equilibrium distances (D), charge transfer (Q_T) and energy gap (E_g) for the BNNT—CO_2 for both considered chiralities. As it is shown, the optimized configurations present small values of adsorption energies and large equilibrium distances, which indicate that the interaction between the carbon dioxide molecule and the pristine boron nitride nanotube is of a physical adsorption nature. In this case, the interaction is

known to be mediated by Van der Waals type interactions. A comparison of values obtained for E_{ads} between the (5,5) and (10,0) tubes highlights a small difference of 0.02eV. This fact suggests a slight tendency of the molecule to interact better with the zigzag rather than with the armchair pristine nanotube.

The charge analysis, carried out through the Mulliken method, suggests that about $0.61e$ and $0.54e$ are transferred from the boron atom to the adjacent nitrogen atom in the (5,5) and (10,0) BNNTs, respectively. This fact endorses the partially ionic character of the B—N bond in BNNTs. By using a Density of States (DOS) analysis, our results also indicate the presence of band gap of 4.35eV and 4.03eV for the (5,5) and (10,0) nanotubes, respectively. These results are in agreement with previous data present in the literature[13,28]. From Table I, we also note that no appreciable energy gap difference is observed for the BN nanotubes. This is an indication that the physical adsorption does not affect the electronic properties of pristine BNNTs. It is important to remark that these results are consistent to the fact that pure BNNTs are quasi-inert structures. Indeed, the low values observed for the interaction energies is a measure of the high stability of these materials without defects[2].

B. BN nanotubes with vacancy-type defect

As it was obtained a weak interaction (between the pristine nanotube and the carbon dioxide molecule), we intent to verify whether or not a vacancy-type defect can favor the adsorption phenomena. In order to do so, first a previous analysis of this kind of defect on the nanotube itself must be performed. This subsection is devoted to understand the effects of a vacancy defect over the geometrical and electronic properties of BNNTs. The vacancy defect was carried out by a vacant boron or nitrogen atom from the nanotube lattice. We also compare the behavior between boron vacancy, which is denoted by BNNT(5,5)V_B and BNNT(10,0)V_B, and nitrogen vacancy, BNNT(5,5)V_N and BNNT(10,0)V_N, nanotubes in terms of geometrical and electronic properties.

We present, on Figure 2, the optimized geometries for the vacancy defect BNNTs. The geometry deformation due to the vacant atom site is shown for all structures. Figure 2a suggests a stretching on the radial direction for the BNNT(5,5)V_B in the region of the removed boron atom. One can note that the relaxation induces a displacement of a nitrogen atom (N_{21}) toward the tube and of two other nitrogen atoms, N_{23} and N_4, outside the tube. In this case, we observed a formation of a 12-fold ring, without new bonding types involving nitrogen close to the vacancy due to the dangling bond. The equilibrium distance between nitrogen atoms were found to be: 2.67 $\mathring{A}$ for N_{23} — N_4, 2.38 $\mathring{A}$ for N_{23} — N_{21} and 2.38 $\mathring{A}$ for N_{21} — N_4. These values indicate that, indeed, no new bonding was established between the nitrogen atoms.

Figure 2b concerns the effect of nitrogen vacancy instead of the boron of Figure 2a. In this case, one can see that deformations appeared in a smaller scale than in the previous case. The two-coordinated boron atom B_{20} relaxes outside the tube whereas the opposite happens for both B_{22} and B_{39}. As can be seen, the formation of new bonding between atoms B_{22} and B_{39} takes place, thus altering the original hexagon lattice around the vacancy site. The distance between the aforementioned boron atoms (B_{39} — B_{22}) is of 1.82 $\mathring{A}$, which corresponds to the formation of a five-fold and nine-fold adjacent rings arrangement. It is important to remark that these geometrical results for vacancy defect BNNT(5,5) are in agreement with other previous results from the literature[14].

Switching to the zigzag chirality, Figure 2c represents the BNNT(10,0)V_B case. A pronounced radial deformation is observed around the vacancy site. Atom N_{39} is displaced outside the nanotube, whereas atoms N_{77} and N_{41} are inward nanotube. Also, a local rebuilding of the bonding between nitrogen atoms N_{77} and N_{41} takes place, thus promoting changes on the original hexagon lattice. The bond distance between nitrogen atoms N_{77} — N_{41} is of 1.46 $\mathring{A}$, thus being responsible for the formation of a five-fold and nine-fold adjacent rings arrangement.

The smaller level of geometrical deformation was observed to take place for the BNNT(10,0)V_N, as can be seen in Figure 2d. A weak bonding is observed between boron atoms B_2 and B_{38}. The bonding length was of 1.78 $\mathring{A}$, which also results in the formation of five-fold and nine-fold adjacent rings. It can be seen that both the binding boron atoms are dislocated inward the nanotube, whereas the two-coordinated boron atom B_{79} is pushed outward the nanotube. We must, again, stress that these results obtained for the vacancy defect of BNNT(10,0) are in agreement with the previously published work[29]. We thus conclude, by analyzing Figure2, that for both BNNT(5,5) and BNNT(10,0), the vacancy formation of boron atom causes higher structural deformation than the nitrogen vacancy.

These geometrical distortions result in important modifications on the nanotubes electronic properties. Figure 3 represents the DOS due to the vacancy defect type. We emphasize that this kind of defect induces impurities states near to the Fermi level in all cases.

For the BNNT(5,5)V_B a final state in the valence band reduced the original band gap to 2.85eV. For the BNNT(5,5)V_N, the appearing of an isolated state between the end of the valence band and the beginning of the conduction band due to the vacancy formation creates a state of 1.37eV near the valance band. The zigzag BNNT(10,0) presents the same trend on the electronic behavior changes when vacancy defect of its armchair counterpart. A final

state inside the original gap of BNNT(10,0)V_B at 2.11eV near the valence band. BNNT(10,0)V_N, on the other hand, presents an isolated state between the end of the valence band and the beginning of the conduction band, 0.97eV close to the valence band.

The charge density analysis also reveals important information related to vacant BNNTs. Figure 4a shows that in the case of BNNT(5,5)V_B, the charge is concentrated over the aromatic ring, particularly above the nitrogen with dangling bonds (N_{23}, N_4 and N_{21}). For the BNNT(5,5)V_N (Figure 4b), one can observe a higher charge concentration over the B_{39} and B_{22} bonds.

For the BNNT(10,0)V_B (Figure 4c), the charge is also mainly concentrated over the two coordinated N_{39} nitrogen atom. It is important to note that, although the presence of the bonding between atoms N_{41} and N_{77}, Figure 4c does not reveal a significant charge concentration between these nitrogen species that would favor strong interaction in bound systems. BNNT(10,0)V_N (Figure 4d), similar to BNNT(5,5)V_N, presents a high concentration of charge over the B_{38}—B_2 bond. These results show that for both chiralities, the variation of charge distribution occurs on the vacancy region. It also demonstrates that the vacancy of a nitrogen atom induces a region with excess of electron whereas the one that is due to boron causes a deficiency of electrons. Therefore, the electrostatic behavior of these defects can be useful for the capture of molecular species.

C. Vacant BN Nanotubes Interacting with CO_2 Molecule

After the optimization and analysis of vacant BNNTs, the goal was to investigate the interaction of these species with the CO_2 molecule. The equilibrium configurations are shown in Figure 5, in which we can note a symmetry breaking of the carbon dioxide molecule related to its original state.

Table II presents the comparison between E_{ads}, D, E_g and Q_T for the different vacancy defect BNNTs interacting with the CO_2 molecule. Considering the BNNT(5,5)V_B—CO_2 (Figure 5a), CO_2 is interacting with the nanotube through a C — N bond, whose length is of 1.40 $\AA$. In this case, the CO_2 molecule presents an inner angle of 118.4^o, with the C — O distances being altered to 1.20 $\AA$ and 1.36 $\AA$. The binding energy between the carbon dioxide molecule and BNNT(5,5)V_B is of -4.42eV (Table II) suggesting that the interaction is of a chemical adsorption nature. Adsorption energies obtained for CO_2 in(8,0) BNNT with a boron antisite (BN) using PAW-PBE[30] are smaller than the obtained with vacancy formation. The charge transfer is of 0.6e and occurs from the carbon to the nitrogen atom due to electronegativity differences. In the interesting case of BNNT(5,5)V_N-CO_2 we observe that a complete dissociation of the CO_2 molecule takes place. The final product is an oxygen atom and a carbon monoxide (CO) molecule. In this case, the binding energy was not included due to the carbon dioxide dissociation. Additionally, these investigations of CO_2-BNNT interactions may provide insight into the mechanism and surface characterization on nanotube planes, for the application of CO_2 storage, for screening and designing of materials for CO_2 capture and how the dissociation may affect the partial charge distribution of the vacancy sites[31–33].

As can be seen in Figure 5b, the dissociated oxygen atom end up binding to the three boron atoms in the vacancy region, thus yield an average B—O bond length of approximately 1.50 $\AA$. The substitutional energy of an oxygen atom in the (5,5) BN nanotube was calculated from the chemical potentials ($E_{sub} = E_{BNNT+O}$ - E_{BNNT} - νO + νN), thus the covalent bond between the oxygen and the boron atoms is of about -13.46eV, thus being of the same order of magnitude as that of the B—N bond on the nanotube. Interestingly, the CO molecule rather than being separated from the nanotube lattice, turns out to interact with the BNNT(5,5)V_N through a relatively weak bond estimated to be about 0.8eV, which characterizes a physisorption process. An evidence of the weak interaction between the CO molecule and the BN nanotube is that the C—O distance preserves the same 1.15 $\AA$ value of the free specie. It is important to remark that experimental studies present in the literature[16] has dealt with a similar situation about the dissociation, albeit in other scope of a graphene type sheet with a boron vacancy interacting with a CO_2 molecule. It was reported that CO_2 molecule suffered decomposition in such a way that the carbon atom was bound to the nitrogen of the sheet, whereas a formed oxygen molecule maintained a weak interaction with the BN sheet[16]. Although in our work this process took place for a nitrogen vacancy system, these theoretical results confirm that dissociation phenomena can indeed be observed experimentally.

For the BNNT(10,0)V_B-CO_2, Figure 5c shows that the interaction with CO_2 results in the breaking of the weak bond between N_{41} and N_{77}. In this case, the CO_2 molecule was linked to the tube by means of a bond between the carbon atom and the N_{41} as well as of another bond between the oxygen and N_{39}. The C — N_{41} presents a bond length of 1.40 $\AA$ whereas the O – N_{39} is of about 1.38 $\AA$. The inner angle of CO_2 in this configuration was found to be of 116.4^o, and the distances are of 1.20 $\AA$ and 1.36 $\AA$. The obtained binding energy between the CO_2 molecule and BNNT(10,0)V_B was of -4.26eV, thus suggesting that this interaction is also of a chemisorption nature. For the BNNT(10,0)V_N-CO_2 (Figure 5d), it was observed a bond breaking between sites B_2 — B_{38} and the rise of two bonds between the CO_2 molecule and BNNT(10,0)V_N. Interactions between carbon atom and B_{38} and another between

oxygen atom and B_{79} were observed. In this configuration the C – B_{38} distance was found to be of 1.64 $\AA$ and the O — B_{79} of 1.37 $\AA$. The inner angle of the molecule changes to 120.2^o and the C—O distances were altered to 1.20 $\AA$ and 1.35 $\AA$. In this case, it is possible to note that the oxygen binding to the boron atom in the nanotube is closer than the carbon. The binding energy was observed to be of -6.53eV, which also suggest a chemisorption interaction between the molecule and BNNT(10,0)V_N.

These results suggests that BNNT(5,5)V_B is more suitable to capture CO_2 than BNNT(5,5)V_N, since while the former interacts with the molecule by means of a chemical adsorption, the later interaction yields the decomposition of the molecule to carbon dioxide molecule, which is highly toxic. Regarding chirality effects, we note that both zigzag nanotubes (BNNT(10,0)V_B and BNNT(10,0)V_N) capture the CO_2 molecule through a chemisorption process. In this case the adsorption energy of the BNNT(10,0)V_N—CO_2 complex is observed to be 2.27eV larger than that of BNNT(10,0)V_B—CO_2. Thus, a system derived from the boron vacancy is showed to be more efficient as far as the carbon dioxide adsorption is concerned.

By comparing the binding energy of the zigzag and the armchair nanotubes, one concludes that the kind of defect plays an important role on the adsorption energy. Although BNNT(5,5)—CO_2 presents only a slight difference of 0.16eV from BNNT(10,0)—CO_2 on the complex binding energy, when the structures are vacancy defect this difference largely increases. Specifically, the adsorption energy is 2.11eV greater for the BNNT(5,5)V_B—CO_2 than for BNNT(10,0)V_N-CO_2.

Table II also shows the charge transfer between the tubes and the CO_2 molecule. We can note that in the case of the vacancy on the boron site, the nanotube presents a charge deficient region, in such a way that the carbon dioxide molecule behaves like a n-type dopant. On the other hand, when the vacancy occurs on a nitrogen site, the BNNT presents an excess of charge, in which case the carbon dioxide molecule behaves like a p-type dopant.

In order to exploit the adsorption effects of the CO_2 molecule over the electronic properties of vacancy defect BNNTs, we plotted the density of states due to the molecule adsorption in Figure 6. It can be observed that, in the case of BNNT(5,5)V_B, the absence of electronic state at the end of the valence band occurs after the adsorption of the CO_2 molecule. Also, the associated gap is observed to be of 3.41eV. In the case of BNNT(5,5)V_N, despite the molecule decomposition, a state near the conduction band remains present, which yields an associated gap of 2.65eV.

For both BNNT(10,0)V_B-CO_2 and BNNT(5,5)V_B-CO_2 a vanishing of a state at the end of the valence band occurs, which yields a gap of 2.14eV. A state between the valence and conduction bands of BNNT(10,0)V_N suffers a small shift of 1.31eV. Table II presents an expected gap for all the analyzed structures. Figure 7 plots the charge density in order to show the charge concentration in the interaction between BNNTs and CO_2 molecule. We observe that CO_2 was bound exactly on the vacancy region with those atoms that present dangling bonds.

IV. CONCLUSIONS

In this work, we performed first-principles calculations to study the interaction of CO_2 molecule with the external surfaces of pristine and vacancy defect armchair (5,5) and zigzag (10,0) boron nitride nanotubes. We observe that, carbon dioxide molecule interacts weakly with pure BNNTs through van der Waals type interactions. Considering vacancy defects of BNNTs we observe that conformational changes on the hexagonal lattice results on changes on the electronic properties that, in turn, result in a greater reactivity with the CO_2 molecule. We observed excellent adsorption energies that points toward a chemisorption state between BNNTs and the CO_2 molecule in most cases. It was also observed a decomposition reaction of the CO_2 molecule when interacting with BNNT(5,5)V_N. In this case, as an oxygen atom remains trapped to the lattice, it is forming a carbon monoxide molecule. By analyzing the adsorption energies and comparing with other values present in the literature, we conclude that the methodology presented in this paper provides an efficient route to obtain reliable CO_2 sensors.

V. ACKNOWLEDGEMENTS

The authors gratefully acknowledge the financial support from the Brazilian Research Councils CNPq, CAPES, FINATEC and FAPDF.

[1] Rubio, A.; Corkill, J. L.; Cohen, M. L. *Phys. Rev. B*, **1994**, 49, 5081.
[2] Chopra, N. G.; Luyken, R. J.; Cherrey, K.; Crespi, V. H.; Cohen, M. L.; Louie, S. G.; Zettl, A. *Science*, **1995**, 269, 966.
[3] Anota, E. C.; Cocoletzi, G. H.; *J. Mol. Model*, **2013**, 19, 2335.

[4] Arenal, R.; Stephan, O.; Kociak, M.; Taverna, D.; Loiseau, A.; Colliex, c.; *Phys. Rev. Lett*, **2005**, 95, 127601.
[5] Bengu, E,; Marks, L. D.; *Phys. Rev. Lett.*, **2001**, 86, 2385.
[6] Suryavanshi, A. P.; Yu, M.; Wen, J.; Tang, C.; Bando, Y. *Appl. Phys. Lett.*, **2004**, 84, 2527.
[7] Zhi, C.; Bando, Y.; Tang, C.; Golberg, D. *Mater. Sci. Eng. R-Rep.*, **2010**, 70, 92.
[8] Cumings, J.; Zettl, A. *Solid State Comm.*, **2004**, 129, 661.
[9] Iijima, S. *Nature*, **1991**, 354, 56.
[10] Bettinger, H. F.; Dumitrica, T.; Scuseria, G. E.; Yakobson, B. I. *Phys. Rev. B*, **2002**, 65, 41406.
[11] Zobelli, A.; Ewels, C. P.; Gloter, A.; Seifert, G.; Stephan, O.; Csillag, S.; Colliex, C. *Nano Lett.*, **2006**, 6, 1955.
[12] Li, J.; Xiao, X.; Xu, X.; Lin, J.; Huang, Y.; Xue, Y.; Jin, P.; Zou, J.; Tang, C. *Scientific Reports*, **2013**, 3, 3208.
[13] Piquini, P.; Baierle, R. J.; Schmidt, T. M.; Fazzio, A. *Nanotechnology*, **2005**, 16, 827.
[14] Li, X. M.; Tian, W. Q.; Huang, X. R.; Sun, C. C.; Jiang, L. *J. Nanopart. Res.*, **2009**, 11, 395.
[15] Montzka, S. A.; Dlugokencky, E. J.; Butler, J. H. *Nature*, **2011**, 476, 43.
[16] Jiao, Y.; Du, A.; Zhu, Z.; Rudolph, V.; Lu, G. Q.; Smith, S. C. *Catal. Today*, **2011**, 175, 271.
[17] Accelrys Software Inc., Discovery Studio Modeling Environment, Release 3.5, San Diego: Accelrys Software Inc., **2012**.
[18] Delley, B. *J. Chem. Phys.*, **1990**, 92, 508.
[19] Perdew, J. P.; Burke, K.; Ernzerhof, M. *Phys. Rev. Lett.*, **1996**, 77, 3865.
[20] Perdew, J. P.; Chevary, J. A.; Vosko, S. H.; Jackson, K. A.; Pederson, M. R.; Singh, D. J.; Fiolhais, C. *Phys. Rev. B*, **1992**, 46, 6671.
[21] Zhao, J. -X,; Ding, Y. -H. *J. Phys. Chem. C*, **2008**, 112, 20206.
[22] Inada, Y.; Orita, H. *J. Comp. Chem.*, **2008**, 29, 225.
[23] Weinert, M.; Davenport, J. W. *Phys. Rev. B*, **1992**, 45, 13709.
[24] Pulay, P. *J. Comput. Chem.*, **1982**, 3, 556.
[25] Paura, E. N. C.; Cunha, W. F.; Neto, P. H. O.; Silva, G. M.; Martins, J. B. L.; Gargano, R. *J. Phys. Chem. A*, **2013**, 117, 2854.
[26] Hirshfeld, F. L. *Theor. Chem. Acc.*, **1977**, 4, 129.
[27] Li, Y.; Zhou, Z.; Zhao, J. *Nanotechnology*, **2008**, 19, 15202.
[28] Wang, S. F.; Zhang, Y.; Zhang, J. M.; Xu, K. W.; Vicent, J. *Appl. Phys. A*, **2012**, 109, 601.
[29] Kang, H. S. *J. Phys. Chem. B*, **2006**, 110, 4621.
[30] Choi, H.; Park, Y. C.; Kim, Y. -H.; Lee, Y. S. J. *Am. Chem. Soc.*, **2011**, 133, 2084.
[31] Lee, K-J; Kim, S-J. *Bull. Korean Chem. Soc.*, **2013**, 34, No. 10.
[32] Liu, Y. G.; Wilcox, J. *Environ. Sci. Technol.*, **2011**, 45, 809.
[33] Silva-Tapia, A. B; Garcia-Carmona, X.; Radovic, L. R. *Carbon*, **2012**, 50, 1152.

FIGURE CAPTIONS

FIG. 1: Frontal and side view of the equilibrium configurations for the CO_2 molecule related to BNNTs (a) and (b) BNNT(5,5); (c) and (d) BNNT(10,0). The blue atoms represent nitrogen, the pink atoms represent boron, the red atom is for the oxygen and carbon is the gray atom.

FIG. 2: Frontal and side view for the optimized geometries of the vacancy defect BNNTs. (a) BNNT(5,5)V_B, (b) BNNT(5,5)V_N, (c) BNNT(10,0)V_B, (d) BNNT(10,0)V_N. The blue atoms represent nitrogen, the pink atoms represent boron, the red atom is for the oxygen and carbon is the gray atom.

FIG. 3: DOS of BNNT(5,5) at the left and BNNT(10,0) at the right for pristine and vacancy defect BNNTs with boron and nitrogen vacancies.

FIG. 4: Charge density of vacancy defect BNNTs. (a) BNNT(5,5)V_B, (b) BNNT(5,5)V_N, BNNT(10,0)V_B, BNNT(10,0)V_N.

FIG. 5: Frontal and side view for the optimized CO_2 configurations on the vacancy defect BNNTs. (a) BNNT(5,5)V_B, (b) BNNT(5,5)V_N, (c) BNNT(10,0)V_B, (d) BNNT(10,0)V_N. The blue atoms represent nitrogen, the pink atoms represent boron, the red atom is for the oxygen and carbon is the gray atom.

FIG. 6: DOS of BNNT(5,5) at the left and BNNT(10,0) at the right for pristine and vacancy defect BNNTs with adsorbed CO_2 molecule.

FIG. 7: Charge density of vacancy defect BNNTs with adsorbed CO_2 molecule. (a) BNNT(5,5)V_B, (b) BNNT(5,5)V_N, (c) BNNT(10,0)V_B, (d) BNNT(10,0)V_N.

TABLE I: Results for the CO_2 adsorption on the pristine (5,5) and (10,0) BNNT optimized geometries.

System	E_{ads} (eV)	D (Å)	E_g (eV)	Q_T (e)
BNNT(5,5)-CO_2	-0.16	3.00	4.35	-0.003
BNNT(10,0)-CO_2	-0.18	2.95	4.03	-0.005

TABLE II: Binding energies and equilibrium distances for the CO_2 adsorption on vacancy BNNT-CO_2 complexes.

System	E_{ads} (eV)	D (Å)	E_g (eV)	Q_T (e)
BNNT(5,5)V_B-CO_2	-4.42	1.40	3.41	-0.50
BNNT(5,5)V_N-CO_2	—	—	2.65	—
BNNT(10,0)V_B-CO_2	-4.26	1.40	2.14	-0.45
BNNT(10,0)V_N-CO_2	-6.53	1.30	1.31	0.82

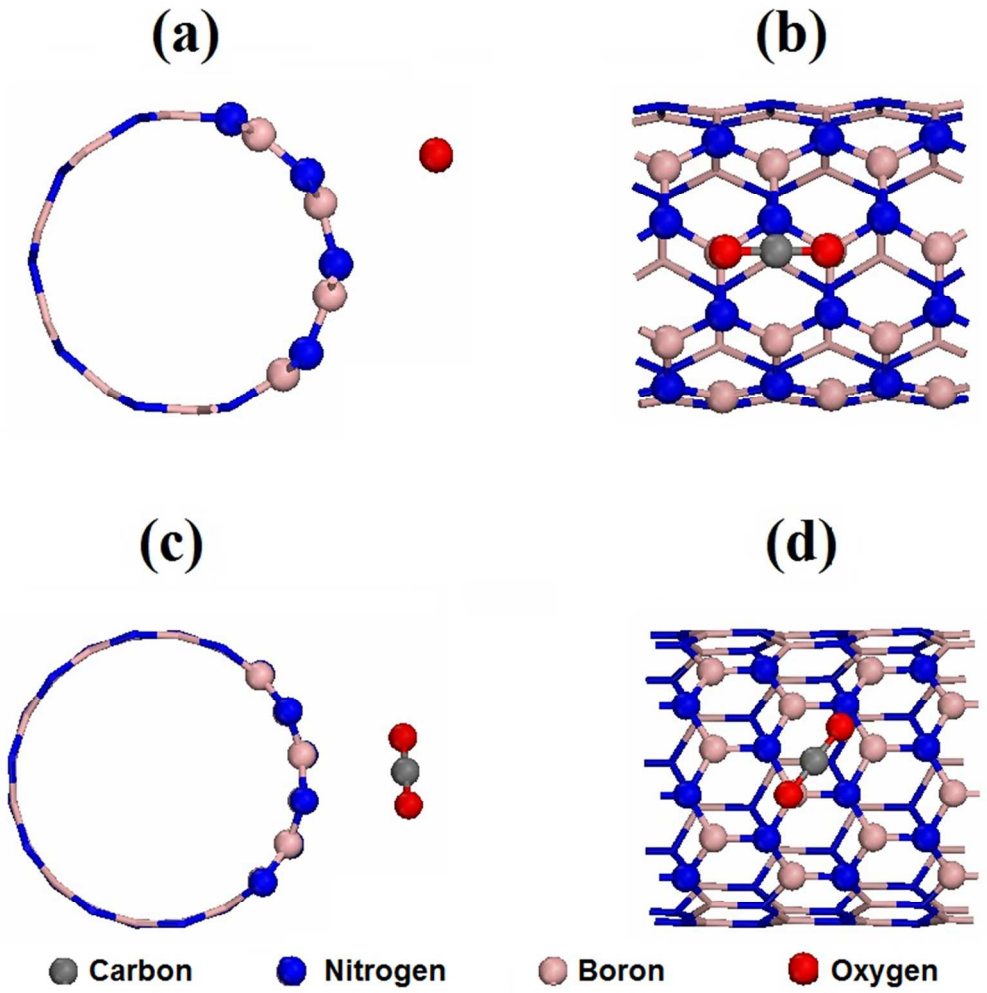

Frontal and side view of the equilibrium configurations for the CO_2 molecule related to BNNTs (a) and (b) BNNT(5,5); (c) and (d)
BNNT(10,0). The blue atoms represent nitrogen, the pink atoms represent boron, the red atom is for the oxygen and carbon is the gray atom.
213x214mm (96 x 96 DPI)

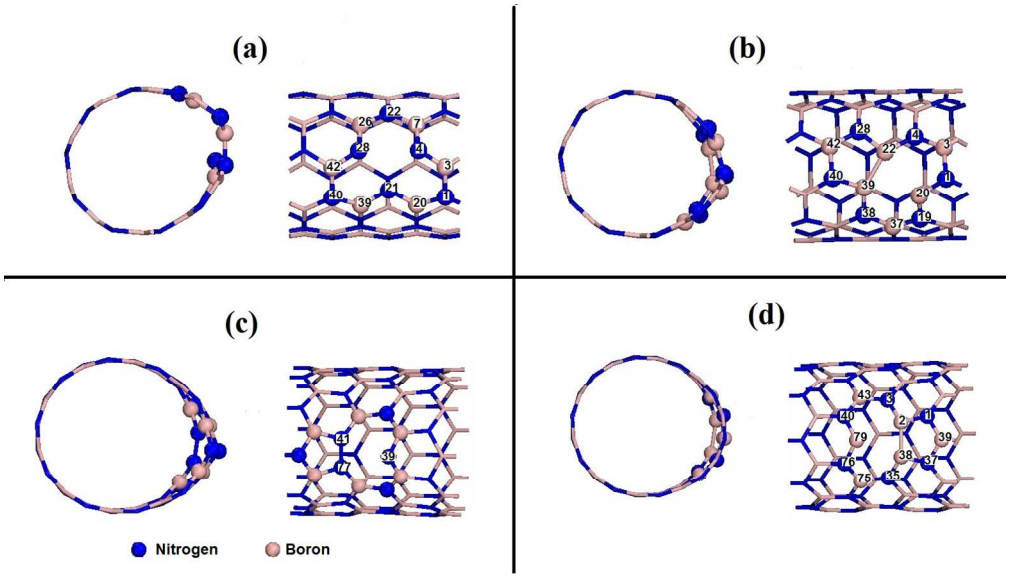

Frontal and side view for the optimized geometries of the vacancy defect BNNTs.
(a) BNNT(5,5)$_B$, (b) BNNT(5,5)$_N$,
(c) BNNT(10,0)V_B, (d) BNNT(10,0)V_N. The blue atoms represent nitrogen, the pink atoms represent boron, the red atom is for the oxygen and carbon is the gray atom.
416x237mm (96 x 96 DPI)

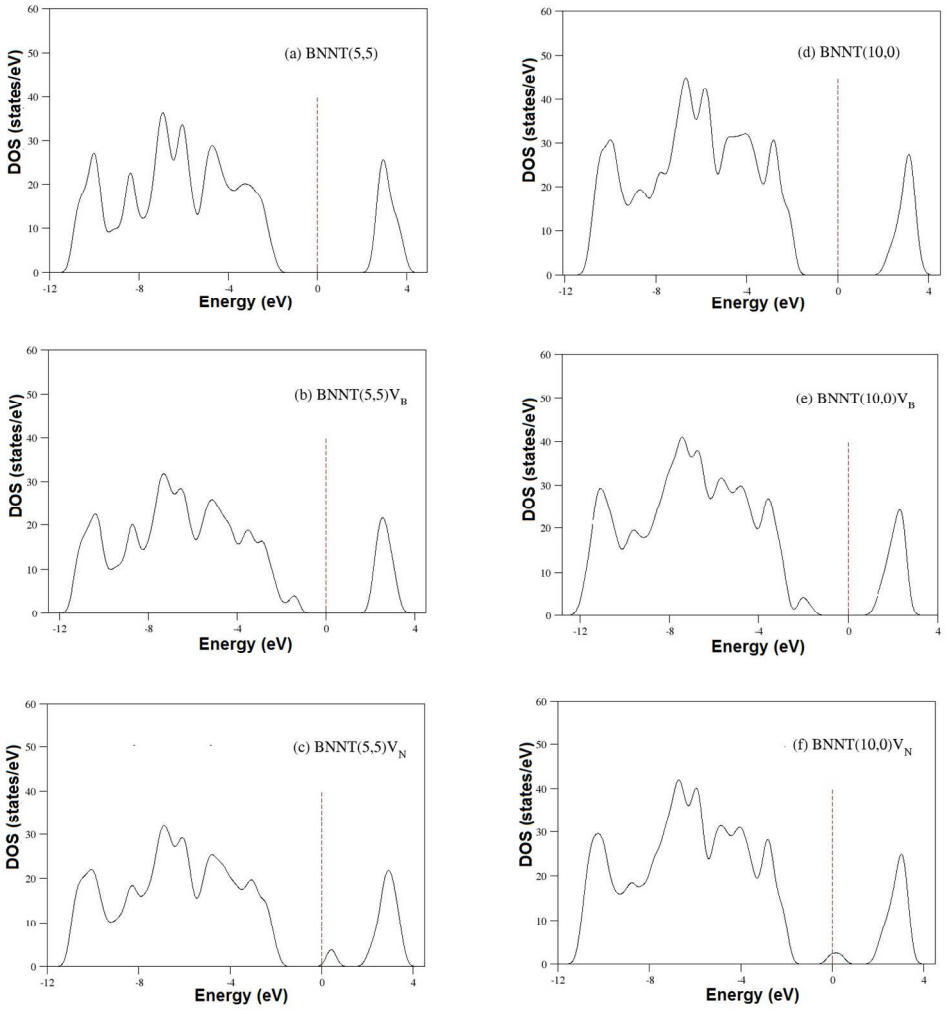

DOS of BNNT(5,5) at the left and BNNT(10,0) at the right for pristine and vacancy defect BNNTs with boron and nitrogen vacancies.
429x449mm (96 x 96 DPI)

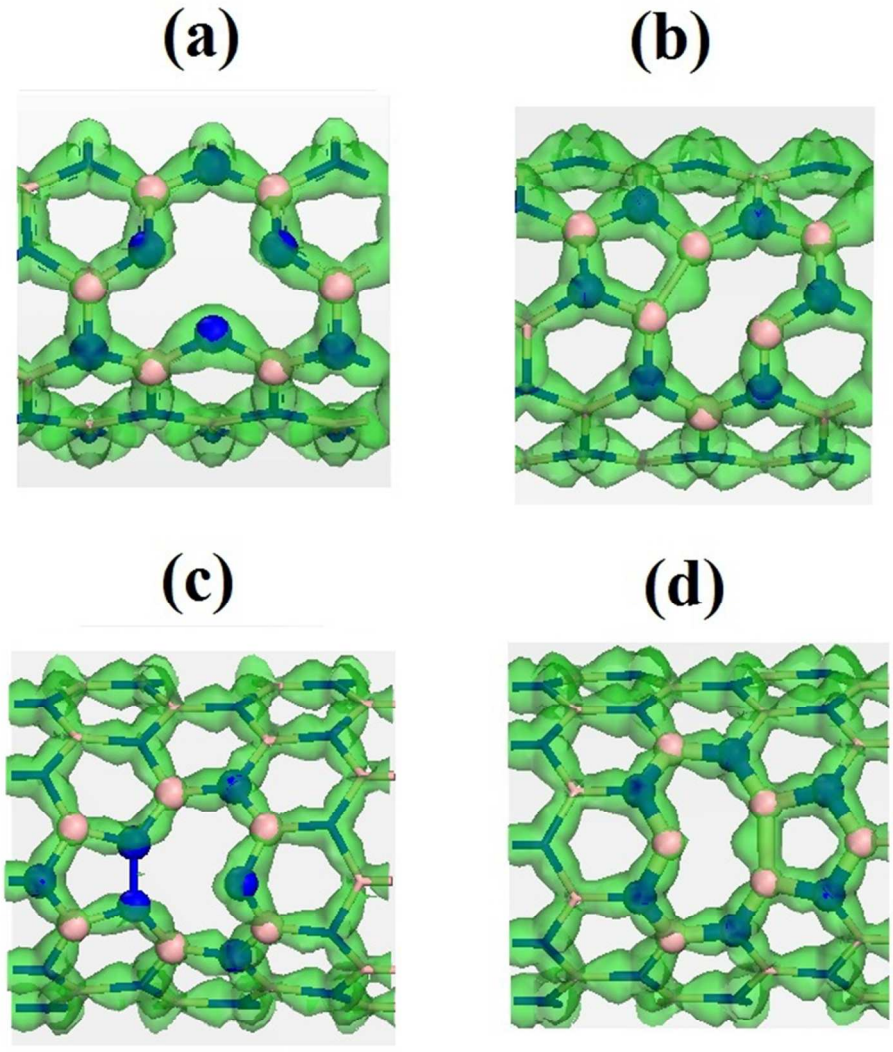

Charge density of vacancy defect BNNTs. (a) BNNT(5,5)V_B, (b) BNNT(5,5)V_N, BNNT(10,0)V_B, BNNT(10,0)V_N.
188x215mm (96 x 96 DPI)

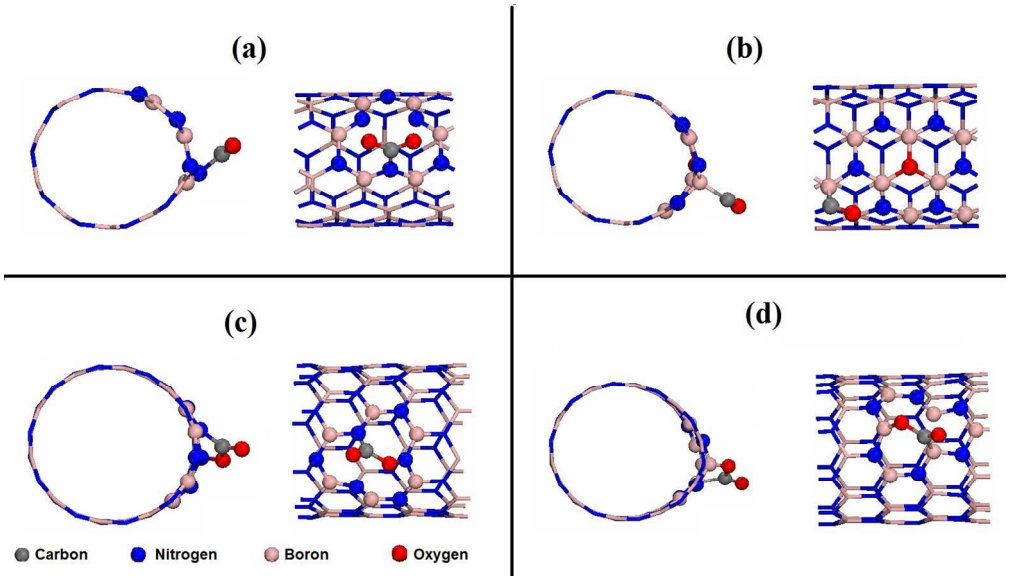

Frontal and side view for the optimized CO_2 configurations on the vacancy defect BNNTs. (a) BNNT(5,5)V_B, (b) BNNT(5,5)V_N, (c) BNNT(10,0)V_B, (d) BNNT(10,0)V_N. The blue atoms represent nitrogen, the pink atoms represent boron, the red atom is for the oxygen and carbon is the gray atom.
418x238mm (96 x 96 DPI)

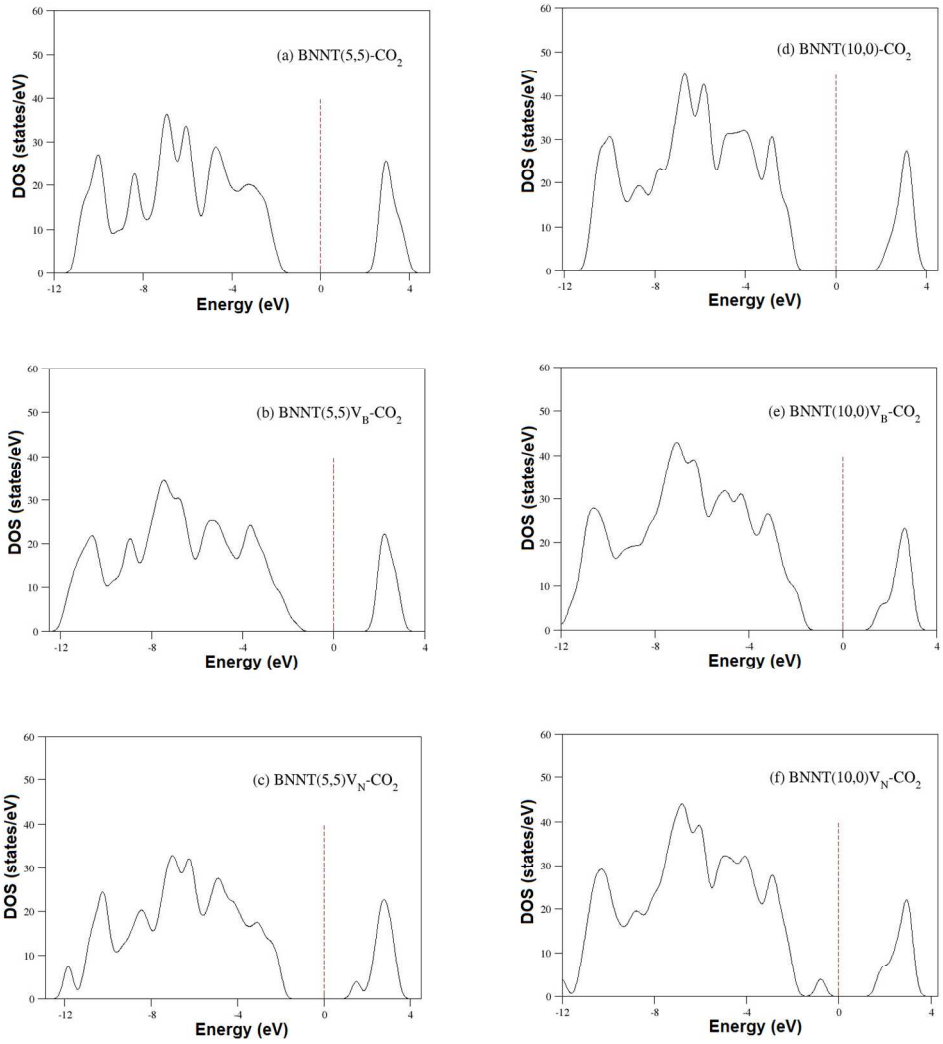

DOS of BNNT(5,5) at the left and BNNT(10,0) at the right for pristine and vacancy defect BNNTs with adsorbed CO_2 molecule.
431x472mm (96 x 96 DPI)

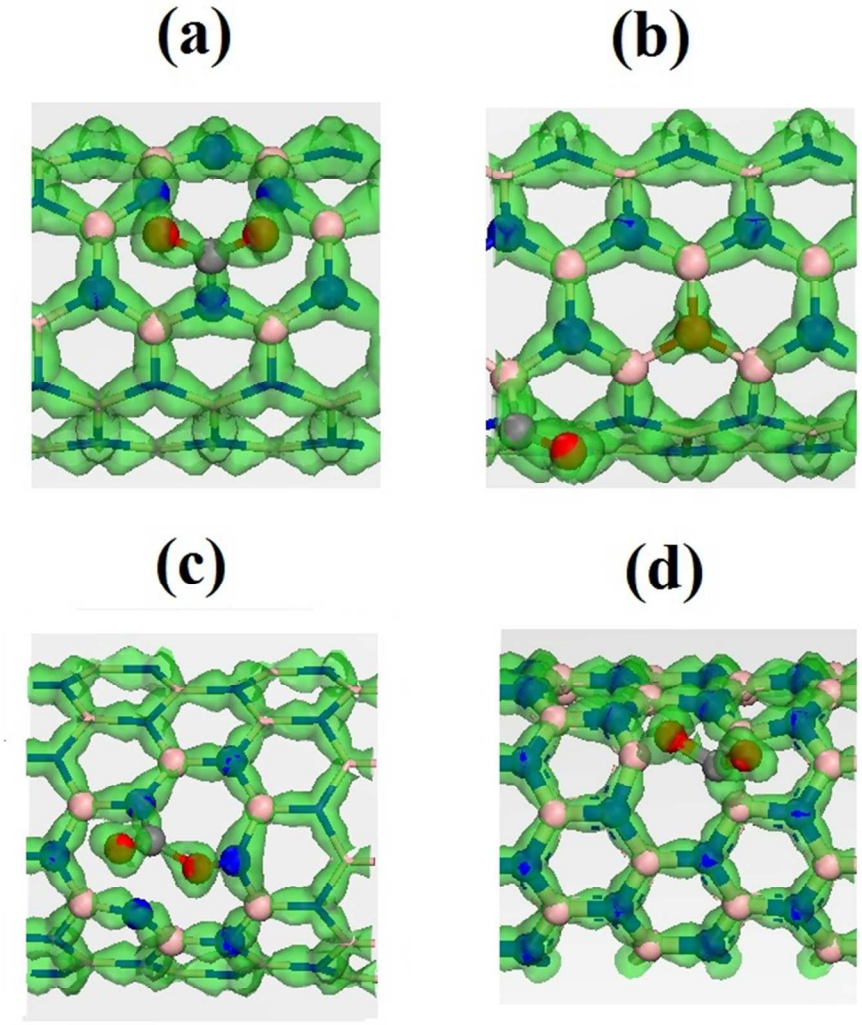

Charge density of vacancy defect BNNTs with adsorbed CO_2 molecule. (a) BNNT(5,5)V_B, (b) BNNT(5,5)V_N, (c) BNNT(10,0)V_B, (d) BNNT(10,0)V_N.
193x214mm (96 x 96 DPI)

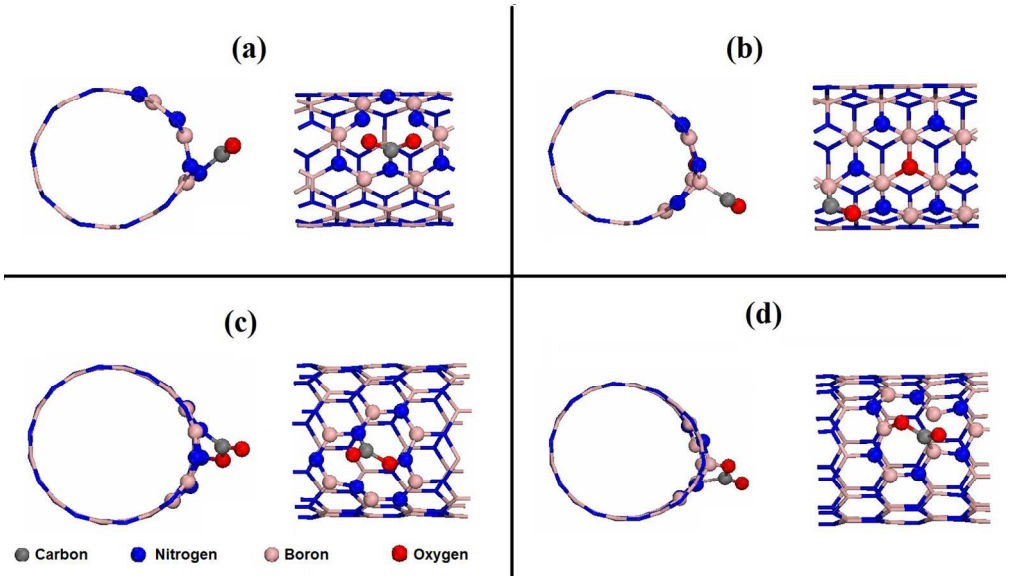

Frontal and side view for the optimized CO_2 configurations on the vacancy defect BNNTs. (a) BNNT(5,5)V_B, (b) BNNT(5,5)V_N, (c) BNNT(10,0)V_B, (d) BNNT(10,0)V_N. The blue atoms represent nitrogen, the pink atoms represent boron, the red atom is for the oxygen and carbon is the gray atom.
418x238mm (96 x 96 DPI)